

# Crisis-induced intermittency in truncated mean field dynamos

Eurico Covas\* and Reza Tavakol†

*Astronomy Unit*

*School of Mathematical Sciences*

*Queen Mary & Westfield College*

*Mile End Road*

*London E1 4NS, UK*

(June 13, 2018)

We investigate the detailed dynamics of a truncated  $\alpha\omega$  dynamo model with a dynamic  $\alpha$  effect. We find the presence of multiple attractors, including two chaotic attractors with a fractal basin boundary which merge to form a single attractor as the control parameter is increased. By considering phase portraits and the scaling of averaged times of transitions between the two attractors, we demonstrate that this merging is accompanied by a crisis-induced intermittency. We also find a range of parameter values over which the system has a fractal parameter dependence for fixed initial conditions. This is the first time this type of intermittency has been observed in a dynamo model and it could be of potential importance in accounting for some forms of intermittency in the solar and stellar output.

## I. INTRODUCTION

Intermittent type behaviour has been observed in a wide range of experimental and numerical studies of dynamical systems. Theoretical attempts at understanding such modes of behaviour fall into two groups: (i) stochastic, involving models in which intermittency is brought about through the presence of some form of external noise and (ii) deterministic, where the mechanism of production of intermittency is purely internal.

Here we concentrate on the latter and in particular on an important subset of such mechanisms referred to as “crisis intermittency” [5,6], whereby attractors underlying the dynamics change suddenly as a system parameter is varied. There are both experimental and numerical evidence for such modes of behaviour (see for example [4,6,7,9] and references therein). As far as their detailed underlying mechanism and temporal signature are concerned, crises come in three varieties [6]. Of particular interest for our discussion here is the type of intermittency (which can occur in systems with symmetry) referred to as “attractor merging crisis”, whereby as a system parameter is varied, two or more chaotic attractors merge to form a single attractor.

An important potential domain of relevance of dynamical intermittency is in understanding the mechanism of production of the so called “grand or Maunder type minima” in solar and stellar activity, during which the amplitude of the stellar cycle is greatly diminished [18]. Many attempts have recently been made to account for such a behaviour by employing various classes of models, including truncated models involving ordinary differential equations (ODE) (c.f. Weiss et al. [17], Zeldovich et al. [19], Spiegel [12]) as well as axisymmetric mean field dynamo models modelled on partial differential equations (PDE), in both spherical shell [11,14,16] and torus [1] topologies. In order to transcend phenomenological explanations and establish the underlying mechanism for such behaviour<sup>1</sup>, it is of vital importance to be able to distinguish between the various intermittency mechanisms and this in turn is greatly assisted by determining the forms of intermittency that can occur for stellar dynamo models.

Here we consider a truncation of an axisymmetric mean field dynamo model and demonstrate that it can possess crisis-induced intermittency. To begin with we find that the system possesses multiple attractors (including two chaotic ones) with fractal basin boundaries, over a wide range of control parameters. We also find parameter intervals over which the system has fractal parameter dependence for fixed initial conditions. Such fractal structures can give rise to a form of fragility (final state sensitivity), whereby small changes in the initial state or the control parameters of the system can result in a different final outcome. We find parameter regions where as the control parameter is varied, the chaotic attractors merge into one attractor thus resulting in crisis-induced intermittency. We verify this

---

\*E-mail: E.O.Covas@qmw.ac.uk

†E-mail: reza@maths.qmw.ac.uk

<sup>1</sup>or behaviours, since after all more than one intermittency mechanism may occur even in a single model but at different system parameters.

by investigating the phase space of the system and calculating the scaling exponent put forward by Grebogi et al. [6]. As far as we are aware, this is the first example of such behaviour in a dynamo model as well as in a 6-dimensional flow.

The structure of the paper is as follows. In section 2 we briefly introduce the model. Section 3 summarizes our results demonstrating the presence of crisis in this model and finally section 4 contains our conclusions.

## II. THE MODEL

The dynamo model considered here is the so called  $\alpha\omega$  mean field dynamo model with a dynamic  $\alpha$ -effect given by Schmalz & Stix [10] (see also Covas et al. [2] for details). We assume a spherical axisymmetrical configuration with one spatial dimension  $x$  (measured in terms of the stellar radius  $R$ ) for which the magnetic field takes the form

$$\vec{B} = \left( 0, B_\phi, \frac{1}{R} \frac{\partial A_\phi}{\partial x} \right), \quad (2.1)$$

where  $A_\phi$  is the  $\phi$ -component (latitudinal) of the magnetic vector potential and  $B_\phi$  is the  $\phi$ -component of  $\vec{B}$ . The model is made up of two ingredients:

(I) the mean field induction equation

$$\frac{\partial \vec{B}}{\partial t} = \nabla \times (\vec{v} \times \vec{B} + \alpha \vec{B} - \eta_t \nabla \times \vec{B}), \quad (2.2)$$

where  $\vec{B}$  is the mean magnetic field,  $\vec{v}$  is the mean velocity,  $\eta_t$  is the turbulent magnetic diffusivity and  $\alpha$  represents the  $\alpha$ -effect.

(II) The  $\alpha$ -effect which arises from the correlation of small scale turbulent velocity and magnetic fields [8] and is important in maintaining the dynamo action by relating the mean electrical current arising in helical turbulence to the mean magnetic field. Here  $\alpha$  is assumed to be dynamic and expressible in the form  $\alpha = \alpha_0 \cos x - \alpha_M(t)$ , where  $\alpha_0$  is a constant and  $\alpha_M$  is its dynamic part satisfying the equation

$$\frac{\partial \alpha_M}{\partial t} = \nu_t \frac{\partial^2 \alpha_M}{\partial x^2} + Q \vec{J} \cdot \vec{B}, \quad (2.3)$$

where  $Q$  is a physical constant,  $\vec{J}$  is the electrical current and  $\nu_t$  is the turbulent diffusivity.

These assumptions allow Eq. (2.2) to be split into the following two equations:

$$\frac{\partial A_\phi}{\partial t} = \frac{\eta_t}{R^2} \frac{\partial^2 A_\phi}{\partial x^2} + \alpha B_\phi, \quad (2.4)$$

$$\frac{\partial B_\phi}{\partial t} = \frac{\eta_t}{R^2} \frac{\partial^2 B_\phi}{\partial x^2} + \frac{\omega_0}{R} \frac{\partial A_\phi}{\partial x}. \quad (2.5)$$

Expressing these equations in a non-dimensional form, relabelling the new variables thus

$$(A_\phi, B_\phi, \alpha_M) \implies (A, B, C), \quad (2.6)$$

and using a spectral expansion of the form

$$A = \sum_{n=1}^N A_n(t) \sin nx, \quad (2.7)$$

$$B = \sum_{n=1}^N B_n(t) \sin nx, \quad (2.8)$$

$$C = \sum_{n=1}^N C_n(t) \sin nx, \quad (2.9)$$

where  $N$  determines the truncation order, reduces the equations (2.3), (2.4) and (2.5) into a set of ODE, the dimension of which depends on the truncation order  $N$ . In Covas et al. [2], the models were taken to be antisymmetric with respect to the equator and it was found that the minimum truncation order  $N$  for which a similar asymptotic behaviour existed was  $N = 4$ . Here in view of computational costs, we take this value of  $N$  for which the set of truncated equations becomes:

$$\frac{\partial A_1}{\partial t} = -A_1 + \frac{DB_2}{2} - \frac{32 B_2 C_2}{15 \pi} + \frac{64 B_2 C_4}{105 \pi} + \frac{64 B_4 C_2}{105 \pi} - \frac{128 B_4 C_4}{63 \pi} \quad (2.10)$$

$$\frac{\partial B_2}{\partial t} = -4 B_2 + \frac{8 A_1}{3 \pi} - \frac{24 A_3}{5 \pi} \quad (2.11)$$

$$\frac{\partial C_2}{\partial t} = -4 \nu C_2 + \frac{16 A_1 B_2}{5 \pi} - \frac{32 A_1 B_4}{7 \pi} + \frac{144 A_3 B_2}{7 \pi} + \frac{416 A_3 B_4}{15 \pi} \quad (2.12)$$

$$\frac{\partial A_3}{\partial t} = -9 A_3 + \frac{DB_2}{2} + \frac{DB_4}{2} - \frac{32 B_2 C_2}{21 \pi} - \frac{64 B_2 C_4}{45 \pi} - \frac{64 B_4 C_2}{45 \pi} - \frac{128 B_4 C_4}{165 \pi} \quad (2.13)$$

$$\frac{\partial B_4}{\partial t} = -16 B_4 + \frac{16 A_1}{15 \pi} + \frac{48 A_3}{7 \pi} \quad (2.14)$$

$$\frac{\partial C_4}{\partial t} = -16 \nu C_4 + \frac{96 A_1 B_2}{35 \pi} + \frac{64 A_1 B_4}{21 \pi} + \frac{32 A_3 B_2}{3 \pi} + \frac{576 A_3 B_4}{55 \pi}, \quad (2.15)$$

where  $D$  is the control parameter, the so called dynamo number, and  $\nu = \frac{\nu_i}{\eta_i}$  which for compatibility with [2,10] we take to be  $\nu = 0.5$ .

Clearly the details of the resulting dynamics will depend on the truncation order chosen. For example, the  $N = 2$  case is expressible as the 3-dimensional Lorenz system and the higher truncations can have different quantitative types of behaviour. The important point, as far as our discussion here is concerned, is that the multi-attractor regime discussed here seems to be present as the order of truncation is increased. In this way such a behaviour might be of potential relevance in understanding some of the intermittent behaviour in the output of the Sun and other stars.

### III. CRISIS-INDUCED INTERMITTENCY

A coarse study of the system (2.10) – (2.15) and higher truncations was reported in [2] from a different point of view. Here we demonstrate the occurrence of crisis-induced intermittency in this system by considering the detailed nature of its attractors, their basins and especially their metamorphoses (merging), while treating  $D$  as the control parameter.

To begin with we recall that symmetries are usually associated with this type of attractor merging. The six dimensional dynamical system considered here possesses the symmetries:

$$A_n \rightarrow -A_n, \quad B_n \rightarrow -B_n, \quad C_n \rightarrow C_n. \quad (3.1)$$

Now assuming the existence of a crisis for this system at  $D = D_c$ , then for crisis-induced intermittency to exist one requires that for  $D < D_c$  there exist two (or more) chaotic attractors and that as  $D$  is increased, the attractors enlarge and at  $D = D_c$  they simultaneously touch the boundary separating their basins. In that case, for  $D$  slightly greater than  $D_c$ , a typical orbit will spend long periods of time in each of the regions where the attractors existed for  $D < D_c$  and intermittently switch between them. An important signature for this mechanism is the way the average time  $\tau$  between these switches scales with the system parameter  $D$ . According to Grebogi et al. [6], for a large class of dynamical systems, this relation takes the form

$$\tau \sim |D - D_c|^{-\gamma}, \quad (3.2)$$

where the real constant  $\gamma$  is the critical exponent characteristic of the system under consideration.

To show that crisis-induced intermittency occurs for the system (2.10) – (2.15), we begin by noting that our numerical results indicate that, for a wide range of parameter values, the system possesses multiple attractors consisting of fixed points, periodic orbits and chaotic attractors. Starting around  $D = 195$ , two cycles coexist and both bifurcate in a doubling bifurcation sequence into two chaotic attractors that coexist after  $D > 203$ . At  $D \approx 200.4$  two other periodic orbits appear which persist for the parameter values considered here. Figures 1 and 2 show these attractors for  $D = 204$ , where all 6 coexist and their positions in the 6-dimensional phase are well separated (note that the apparent overlaps in Figs 1 and 2 are due to projections).

We also found the corresponding basins of attraction for each attractor which indicate fractal boundaries. This can be seen in Figure 3 which shows a two dimensional cut ( $C_2 = A_3 = B_4 = C_4 = 0$ ) of the basin boundary for this

system at the parameter value  $D = 204$  and Figure 4 which shows the magnification of a region of Figure 3 where both chaotic attractors possess fractal basins [20]. We also calculated the box counting dimension of the boundary between attractors on a horizontal 1-D cut of Figure 4, which turned out to be non integer, further substantiating the fractal nature of the boundaries.

Now as  $D$  is increased, the two chaotic attractors merge and give rise to a single connected attractor. Figure 5 shows the time series for the variable  $A_1$  after the merging and Figure 6 shows the projection of the merged attractors on the variables  $A_1$ ,  $B_2$  and  $C_2$ . Prior to  $D_c \approx 204.2796$ , there is no switch between the two attractors and the time series does not show the bimodal behaviour seen in Figure 5.

These results show a clear indication for the occurrence of crisis-induced intermittency in this model. To substantiate this further, we checked that for this system the scaling relation (3.2) is satisfied in the neighbourhood of  $D_c \approx 204.2796$ . Figure 7 shows the plot of  $\log_{10} |\tau|$  versus  $\log_{10} |D - D_c|$ . To produce the plot, 28 points were taken at regular spacings with the initial conditions chosen in the chaotic basin of the merged attractor after  $D \approx 204.2796$  and 200 million iterations were taken for each point. The transitions between the ghosts of the previous attractors were detected using the averages of the variable  $A_1$  over a pseudo-period of approximately  $\Delta t \approx 1.5$  non-dimensional time units. As can be seen the points are well approximated by a straight line, which was obtained using a least squares fit which giving  $\gamma \approx 0.79 \pm 0.03$ .

The  $\gamma$  coefficient can be calculated also from theoretical grounds, as shown in Grebogi et al. [6]. The method involves calculating the stable and unstable manifolds of the unstable orbit (thereafter  $B$ ) mediating the crisis. By examining the trajectories around the transitions between the ghosts of the previous attractors at  $D = 204.35 > D_c$ , we found the point where the orbit went inside the portion of the unstable manifold of the  $B$  that has poked over to the other side of the stable manifold of  $B$ . The orbit then follows closely the orientation of the stable and unstable manifolds. We then calculated an estimate of the direction of the unstable and stable manifolds. Since this was very sensitive, the value of  $\gamma$  had a large error bar, that is, the calculated value could be anywhere on the range  $[0.4, 1.2]$ , depending on minor changes in the choice of the vectors that determine the unstable and stable manifolds. Because the system was high dimensional, all the projections in two dimensional planes we used were not very useful to determine with good precision the directions of the two manifolds. Therefore we were unable to calculate the critical exponent with sufficient precision to compare with the one calculated from the time between flips of the orbit.

Finally we looked at the parameter dependence of the system for fixed initial conditions. We found that there are intervals of  $D$  for which this is fractal. This can be seen from Figure 8 which depicts the final state (attractor) of the system (2.10) – (2.15) as a function of changes in the parameter  $D$  and the initial condition  $B_2$ .

#### IV. CONCLUSIONS

We have found the presence of multiple attractors with fractal basin boundaries as well as crisis-induced intermittency in a truncated axisymmetric  $\alpha\omega$  dynamo model which is antisymmetric with respect to the equator. We have seen that this type of intermittency is due to the collision of the two chaotic attractors and have confirmed this by calculating the scaling coefficient suggested by Grebogi et al. [6].

The presence of crisis-induced intermittency, coupled with the facts that this type of multiple attractors seem to persist in higher order truncations and the presence of symmetry in dynamo models, may indicate the relevance of this type of intermittency in more realistic dynamo settings.

We have also found that this system possesses fractal parameter dependence for fixed initial conditions. The presence of such fractal structures results in a form of fragility (final state sensitivity), whereby small changes in the initial conditions or the control parameter of the system can result in qualitative changes in its final dynamics. This type of sensitivity could be of significance in astrophysics in that, for example, it could potentially lead to stars of same spectral type, rotational period, age and compositions showing different modes of dynamical behaviour [13].

Finally as far as we are aware, this is the first instance of such behaviour in a dynamo model as well as in a  $6D$  flow.

#### ACKNOWLEDGMENTS

We would like to thank John Brooke and Andrew Tworkowski for helpful discussions. We also thank an anonymous referee for his useful comments and criticisms. EC is supported by grant BD / 5708 / 95 – Program PRAXIS XXI, from JNICT – Portugal. RT benefited from PPARC UK Grant No. H09454. This research also benefited from the EC Human Capital and Mobility (Networks) grant “Late type stars: activity, magnetism, turbulence” No. ERBCHRXCT940483.

- 
- [1] Brooke, J.M. and Moss, D., 1995, *A&A*, **303**, 307
- [2] Covas, E., Tworkowski, A., Brandenburg, A. & Tavakol, R., 1997, *A&A*, **317**, 610
- [3] Feudel, F., Jansen, W., and Kurths, J., 1993, *Int. J. Bifurc. Chaos*, **3**, 131
- [4] Ditto, W.L., Rauseo, S., Cawley, R., Grebogi, C., Hsu, G.H., Kostelich, E., Ott, E., Savage, H.T., Seguan, R., Spano, M.L. and York, V.A., 1989, *Phys. Rev. Lett.* **63**, 923
- [5] Grebogi, C., Ott, E., and Yorke, J.A., 1982, *Phys. Rev Lett*, **48**, 1507
- [6] Grebogi, C., Ott, E., Romeiras, F., and Yorke, J.A., 1987, *Phys. Rev A.*, **36**, 5365
- [7] Karakotsou, Ch., and Anagnostopoulos, A.N., 1996, *Physica D*, **93**, 157
- [8] Krause, F. and Rädler, K.-H., 1980, *Mean Field Magnetohydrodynamics and Dynamo Theory*, Pergamon, Oxford
- [9] Ott, E., *Chaos in Dynamic Systems*, 1993, Cambridge Press, Cambridge
- [10] Schmalz, S. and Stix, M., 1991, *A&A*, **245**, 654
- [11] Schmitt, D., Schüssler, M., and Ferriz-Mas, A., 1996, *A&A*, **311**, L1–L4
- [12] Spiegel, E.A. 1994, in Proctor M.R.E., Gilbert A.D., eds, *Lectures on Solar and Planetary Dynamos*, Cambridge Univ. Press, Cambridge.
- [13] Tavakol, R.K, Tworkowski, A. S., Brandenburg, A., Moss, D., and Tuominen, I., 1995, *A&A*, **296**, 269
- [14] Tobias, S.M., 1996, *A&A*, **307**, L21–L24
- [15] Tobias, S.M., Weiss, N.O., and Kirk, V., 1995, *MNRAS*, **273**, 1150
- [16] Tworkowski, A.S., Tavakol, R.K, Brandenburg, A., Moss, D., and Tuominen, I., 1996, *MNRAS*, submitted
- [17] Weiss, N.O., Cattaneo, F., and Jones, C.A., 1984, *Geophys. Astrophys. Fluid Dyn.*, **30**, 305
- [18] Weiss, N.O., in *Lectures on Solar and Planetary Dynamos*, edited by Proctor, M.R.E. and Gilbert, A.D., Cambridge University Press, Cambridge
- [19] Zeldovich, Ya.B., Ruzmaikin, A.A., and Sokoloff, D.D., 1983, *Magnetic Fields in Astrophysics*, Gordon and Breach, New York
- [20] A version of this basin picture in full colour is available at the following web address <http://www.maths.qmw.ac.uk/~eoc/basin.html>

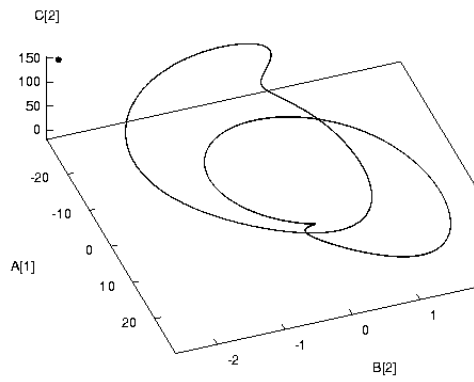


FIG. 1. Phase portraits of the two fixed points and the two stable cycles

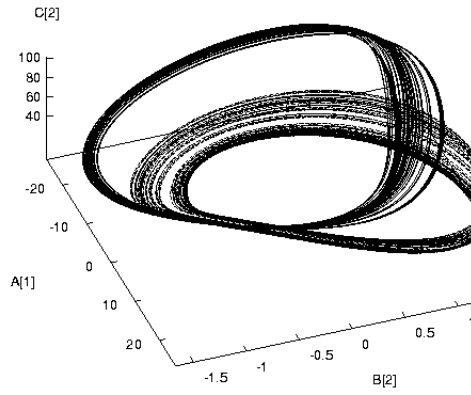


FIG. 2. Phase portraits of the two coexistent chaotic attractors

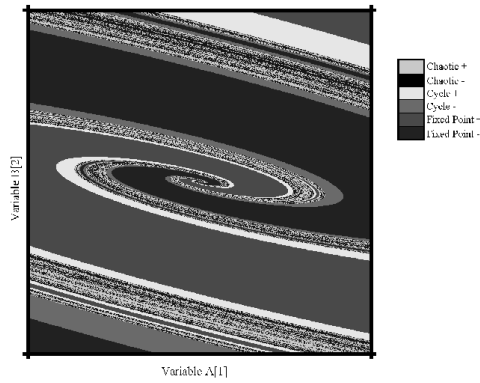


FIG. 3. A  $800 \times 800$  grid showing a 2-D cut of the basins of attraction with  $D = 204$  and  $C_2 = A_3 = B_4 = C_4 = 0$ . Variables  $A_1$  and  $B_2$  were centred at  $(0, 0)$  and the size of the picture is 2 by 1. In the legend, + and - indicate the sign of the time average of  $A_1$

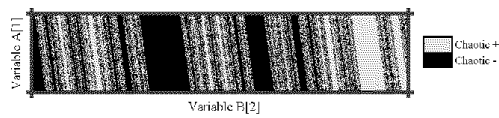


FIG. 4. A  $800 \times 160$  grid showing the amplification of the previous picture (close to the lower left corner) with  $A_1 = -0.804$  and  $B_2 = -0.700$  and with size 0.01 by 0.002

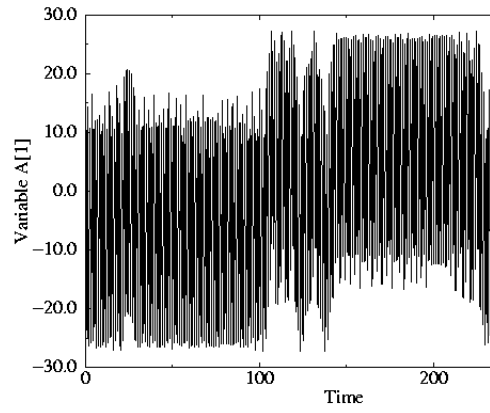


FIG. 5. Chaotic time series for the merged attractors for  $D = 205 > D_c$

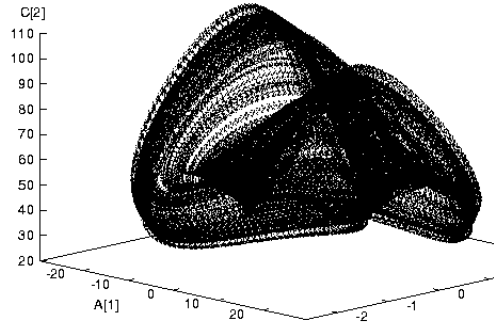


FIG. 6. The projection of the resulting merged chaotic attractor in the space  $A_1, B_2, C_2$  for  $D = 207$

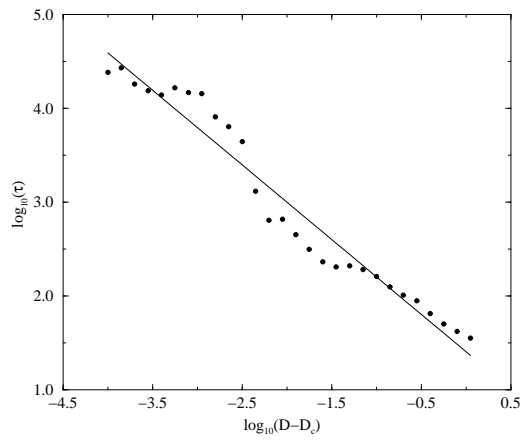


FIG. 7. Scaling of  $\tau$  as a function of the distance to the critical dynamo number  $D_c$  together with the fitted line

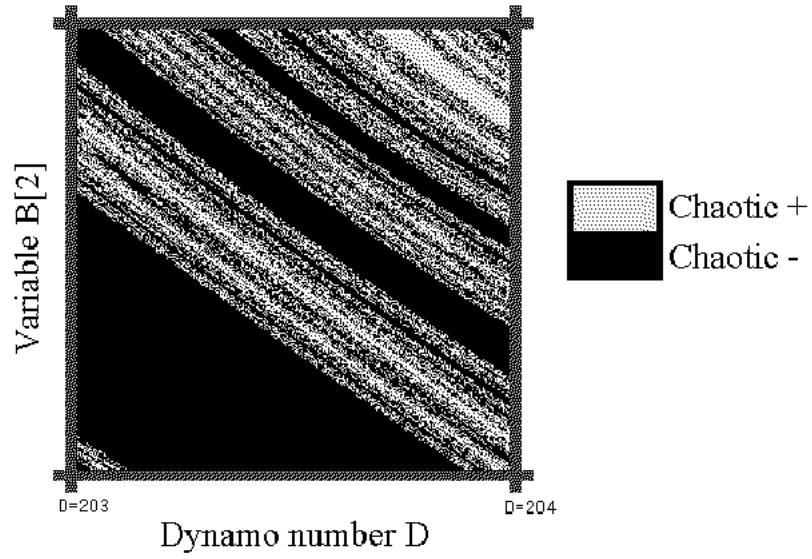


FIG. 8. Depiction of the final state (attractor) of the system as a function of changes in the parameter  $D$  and the initial condition  $B_2$ . This Figure represents a horizontal slice of Fig. 4 for many runs with different dynamo numbers. A resolution of 300 by 300 pixels was used and all initial conditions were taken to be zero except for  $A_1 = -0.80$  and  $B_2$  centred at  $-0.70$